

## A Wide-band Channel Simulation Algorithm for the Suzuki Fading Channel with the Spatial Correlation

Jin Weon Chang\*, Yang Soo Park\*, Ku Yong Ha\*, Hyung Myung Kim\* Regular Members

### 공간적 상관관계를 갖는 광대역 스즈키 페이딩 채널 시뮬레이션 알고리즘

正會員 張眞元\*, 朴洋守\*, 河求容\*, 金炯明\*

#### ABSTRACT

A wide-band channel simulation algorithm for Suzuki fading channel has been proposed in this paper. The proposed algorithm generates the Suzuki fading signal[2] of which the lognormal fading components have the spatial correlation between amplitudes in adjacent profiles and the temporal correlation between paths in a profile. It has been shown that the algorithm can be extended to be applicable in the channel where a diversity receiver is used. The proposed algorithm can be used in the design of urban mobile communication systems as well as the performance evaluation of those systems.

#### 要 約

본 논문에서는 스즈키 페이딩 채널에 대한 광대역 채널 시뮬레이션 알고리즘을 제안하였다. 본 알고리즘은 대수정규 페이딩의 프로파일간에 공간적 상관관계와 한 프로파일내의 경로간의 시간적 상관관계를 갖는 스즈키 페이딩 신호를 생성한다. 제안된 알고리즘은 다이버시티 수신기가 사용되는 채널에 이용될 수 있도록 확장됨을 보였다. 제안된 알고리즘은 이동통신 시스템의 설계와 기존 시스템의 평가에 이용될 수 있다.

---

\* 한국과학기술원 전기 및 전자공학과  
論文番號 : 95042-0203  
接受日字 : 1995年 2月 3日

## 1. Introduction

The signal through a mobile communication channel is essentially contaminated by the multipath fading due to reflection, refraction and scattering by buildings, other man-made obstacles, terrain and etc. The signal components arriving from indirect paths and the direct path, if the direct path exists, combine and produce a distorted version of the transmitted signal. In narrow-band transmission, the multipath medium causes fluctuations in the received signal amplitude and phase. In wide-band pulse transmission, on the other hand, the multipath medium produce a series of delayed and attenuated pulses for every transmitted pulse.

Experimental testing of radiocommunication systems is time consuming and expensive since large amounts of experimental systems and man powers are required to conduct the experiment in accordance with the statistical variation of the mobile channel. It is clearly attractive to simulate systems in the laboratory since conditions can then be tightly controlled, but it is very important to ensure that all the relevant properties of the signal can be adequately simulated. Simulation amounts to produce signals which have appropriate statistical properties.

The concept of modeling the wide-band mobile radio channel is known as a densely tapped delay line<sup>(1)</sup>, which was refined and verified by the extensive sets of measurements<sup>2,3)</sup>. An experimental evidence<sup>(4)</sup> shows that after normalization to remove slow fading effects, the small-scale amplitude variations, particularly for paths with delay less than 1 $\mu$ s, can be very accurately modeled by a Rayleigh distribution. The large-scale variations approximate to a lognormal distribu-

tion, which tends to confirm the assumption made by Turin<sup>(1)</sup>. Thus the fluctuation of path strength in each time-delay cell can be well approximated as uncorrelated Rayleigh fading, superimposed on partially correlated lognormal fading. According to the analysis of measured data<sup>(4)</sup> the average correlation coefficient of Rayleigh fading components is insignificant, but lognormal fading components has considerable value. Realistic simulation requires that the lognormal fading component has the temporal correlation between paths and the spatial correlation between profiles<sup>(3)</sup>.

Hashemi<sup>(3)</sup> used the lognormal distribution to generate all path strengths. One of factors which influence this choice is the need to simulate correlation between successive echo amplitudes in the same profile (temporal correlation) and correlation between amplitudes in successive profiles (spatial correlation). Hashemi took into account both the spatial correlation and the temporal correlation but only for consecutive paths and profiles. A simulation algorithm for the generation of Suzuki fading signal was proposed by Park<sup>(5)</sup>. The algorithm was based on the measured data of Turkmani<sup>(4)</sup>. This algorithm assumed Suzuki fading and considered the temporal correlation between all paths in 1 $\mu$ s, not just between consecutive paths, in the same profile. But the algorithm did not take into account the spatial correlation.

In this paper, we revise the simulation algorithm of Park<sup>(5)</sup> to consider the spatial correlation of lognormal fading component between profiles. The proposed simulation algorithm is extended so that the algorithm is also applicable to the channel where a diversity receiver is used. In the mobile communication systems, the diversity receiver is used

at most base stations<sup>(6)</sup>. The channel effect has been studied for many years when diversity receiver is used<sup>(7,8,9)</sup>.

In chapter II, we describe wide-band channel model and Suzuki fading. The chapter III is written for the revised algorithm with the spatial and temporal correlation of lognormal component and the extended algorithm for diversity receiver. The numerical results and discussion are given in chapter IV. Chapter V contains the concluding remarks.

## II. Wide-band Channel Model and Suzuki Fading

### 1. Wide-band Channel Model

As is well known, the wide-band channel is modeled as a linear filter which is composed of statistically determined parameters. Let  $x(t)$  and  $y(t)$  represent the transmitted signal and the received signal, respectively. Then

$$x(t) = \text{Re}\{s(t)e^{j\omega_0 t}\}, t \in (-\infty, \infty)$$

where  $s(t)$  denotes the complex valued low-pass waveform of the transmitted signal and  $\omega_0$  is the carrier frequency. The received signal will be

$$y(t) = \text{Re}\{h(t) * s(t)\}e^{j\omega_0 t}$$

where the  $h(t)$  denote the impulse response of the Suzuki fading channel which is usually given as

$$h(t) = \sum_{k=1}^N A_k \delta(t-t_k) \exp(j\theta_k) \tag{1}$$

where  $N$  represent the number of paths. The path strength characteristics of the composite path with the given delay is made up by the statistical properties of three parameters in the linear filter model. The parameters are

path strengths  $\{A_k\}_0^{\infty}$ , time delay  $\{t_k\}_0^{\infty}$ , and phase shift  $\{\theta_k\}_0^{\infty}$ . The statistical properties of these parameters are determined and verified through the channel measurement<sup>(2,3,4)</sup>. Path strength can be modeled by Rayleigh distribution or lognormal distribution according to the mobile communications environment. Modified Poisson distribution is fit well for the description of time delay. But fixed time delay is used for a hard-ware simulator practically. The phase shift is usually assumed to be uniformly distributed<sup>(10)</sup>.

The Turin's model<sup>(11)</sup> of equation (1) is quite general and can be used to obtain the response of the channel to any low-pass waveform signal  $s(t)$ . The model is the basis of both a soft-ware simulation of mobile communication channel and a hard-ware<sup>(10)</sup>.

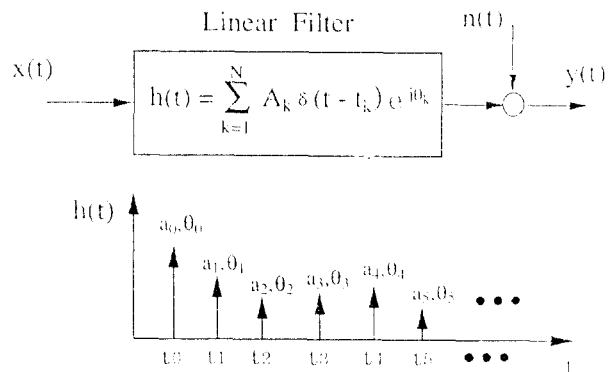


Fig. 1. Wide-band Channel Model.

### 2. Suzuki Distribution

Multipath fading is classified by the statistical properties of path strength into Rayleigh fading (sometimes called as fast fading or short term fading) and lognormal fading (slow fading or long term fading or shadowing). It is generally accepted that fading path strength is Rayleigh distributed over a spatial

dimension of a few hundred wavelength and is lognormally distributed over much larger area. But, this assumption always has variations depending on the particular geography involved. A new distribution is proposed by Suzuki. The distribution is Rayleigh distribution average power of which is lognormally distributed<sup>(2)</sup>. The probability density function (PDF) of Suzuki distribution is expressed as

$$PDF(A) = \int_0^{\infty} PDF_R(A|L) PDF_L(L) dL \quad (2)$$

where  $PDF_R(A|L)$  is the PDF of Rayleigh distribution and  $PDF_L(L)$  is the PDF of lognormal distribution. The PDF of the Rayleigh distribution is given as

$$PDF_R(A|L) = \frac{R}{L} \exp\left(-\frac{R}{L}\right) \quad (3)$$

where  $L$  is the average power of Rayleigh distribution and the PDF of the lognormal is

$$PDF_L(L) = \frac{1}{\sqrt{2\pi} \sigma_L L} \exp\left[-\frac{\{\ln \log_e(L/\lambda)\}^2}{2\sigma_L^2}\right] \quad (4)$$

where  $\lambda$  and  $\sigma_L$  is the mean of lognormal distribution and the variance.  $R$  is Rayleigh dis-

tributed random variable and  $L$  is lognormally distributed random variable.  $A$  is Suzuki distributed random variable, which equals to Rayleigh distributed random variable with lognormally distributed average power. In succeeding chapters, the same notation is used.

### 3. Channel Parameters for Simulation

Turkmani<sup>(4)</sup> suggested parameters of a wide-band multipath fading channel simulator which is composed of a densely tapped delay line. The each tap comprises a Rayleigh modulator, a lognormal modulator, and a weighting. He deduced several informations on wide-band channel simulator from channel measurements. The average correlation coefficient of Rayleigh fading components and that of lognormal fading components were represented. The former is ignorable, but the latter has a considerable value. He suggested that the correlations of the lognormal fading component be considered in a practical hardware channel simulator between only two adjacent taps for simplicity. The mean signal

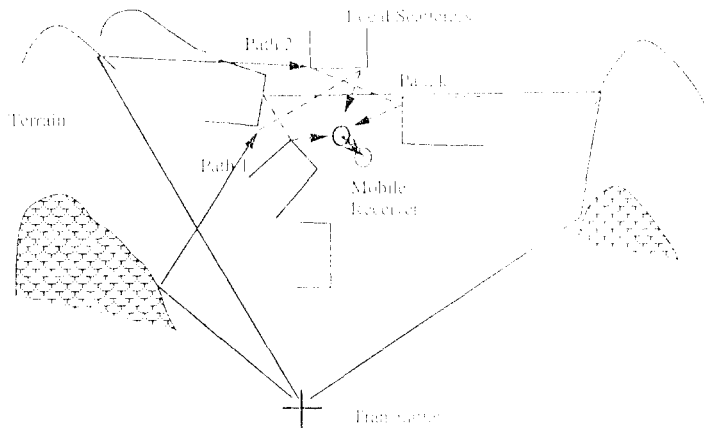
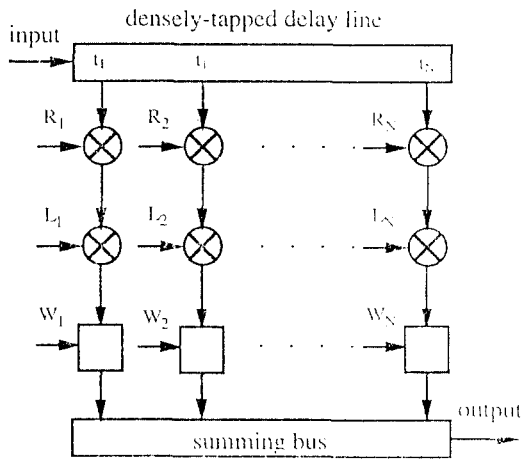


Fig. 2. Wide-band Multipath Channel Effect.

level explicitly indicates the time delay value of each tap which is the most essential for an accurate channel simulation. Fig. 3 shows the schematic diagram of the multipath fading channel simulator. Channel parameters for 12 taps are listed in table 1 and the temporal correlation coefficients of lognormal fading component are listed in table 2 from Turkmani's empirical data.

### III. Algorithm for the Generation of Suzuki Fading Signal



$R_1, R_2, \dots, R_N$  : independent, zero-mean, complex Gaussian  
 $L_1, L_2, \dots, L_N$  : zero-mean lognormal  
 $W_1, W_2, \dots, W_N$  : weighting factors for each tap

Fig. 3. Tapped Delay-line Representation of a Multipath Fading Channel Simulator.

Suzuki fading signal can be well approximated as uncorrelated Rayleigh fading, superimposed on partially correlated lognormal fading<sup>(4)</sup>. The lognormal fading component has the temporal correlation between amplitudes of paths in a profile and the spatial correlation between amplitudes in adjacent profiles according to the movement of receiver<sup>(3)</sup>. The algorithm of Park<sup>(5)</sup> provides no spatial correlation between profiles which is described in the section III.1. If the algorithm is modified to consider the spatial correlation, it can simulate more realistic mobile channel. The modification is given in the section III.2.

Rayleigh fading component has no temporal correlation because it is not affected by the terrain. It has much weaker spatial correla-

Table 2. Temporal Correlation Coefficient of Lognormal Fading Component.

$t_1 - t_k (\mu\text{sec})$	$\rho_l$	$t_1 - t_k (\mu\text{sec})$	$\rho_l$
0.0	1.00	0.6	0.43
0.1	0.66	0.7	0.40
0.2	0.48	0.8	0.37
0.3	0.44	0.9	0.33
0.4	0.41	1.0	0.29
0.5	0.41		

Table 1. Channel Parameters.

k	$t_k [\mu\text{sec}]$	$\sigma_{Lk}$	$\lambda_k$	k	$t_k [\mu\text{sec}]$	$\sigma_{Lk}$	$\lambda_k$
1	0.0	2.0277	1.0000	7	2.0	1.5560	1.1281
2	0.1	1.9253	0.5708	8	2.3	1.8989	0.1297
3	0.4	1.6982	0.2698	9	3.8	1.3122	1.1012
4	0.7	1.8989	0.2304	10	5.9	1.3032	0.0934
5	1.0	1.8578	0.1841	11	9.4	1.4774	0.0985
6	1.6	1.5399	0.1340	12	10.0	1.4876	0.0959

tion than the lognormal fading component. However, when diversity receiver is used, we should consider the spatial correlation of Rayleigh fading component according to antenna spacing. The correlation is larger at the base station than in the mobile, because the received signals at the base station have small arrival angle<sup>(7,8,9)</sup>. The section III.3 of this chapter describes the generation of Rayleigh fading component when a 2-branch diversity receiver is used.

1. The Existing Algorithm for the Generation of Suzuki Fading Signal<sup>(5)</sup>

Rayleigh fading signal becomes Suzuki fading when the average power of Rayleigh fading signal is lognormally distributed<sup>(2)</sup>. To generate Suzuki fading signal, the lognormal fading component has been first generated and then Rayleigh fading component superimposed on the generated lognormal fading component which becomes the average power of Suzuki signals. Suppose  $L_k(n)$  denotes the lognormal fading component at the k-th path in the n-th profile. Then the lognormal fading components in a profile have the temporal correlation,  $\rho_L(k, m)$ , between the paths k and m can be expressed as

$$\rho_L(k, m) = E\{L_k(n)L_m(n)\}/\sigma_{L_k} \sigma_{L_m} \quad \text{for } k, m = 1, 2, \dots, N. \quad (5)$$

The temporally correlated  $L_k(n)$  can be generated from the temporally correlated Gaussian random variables by

$$L_k(n) = \lambda_k e^{X_k(n)} \quad (6)$$

where  $\lambda_k$  is the mean of  $L_k(n)$  and  $X_k(n)$  denotes the Gaussian random variable and  $\rho_X(k, m)$  denotes the temporal correlation of that.

Then the relationship between  $\rho_L(k, m)$  and  $\rho_X(k, m)$  is given by

$$\rho_X(k, m)\sigma_{X_k}\sigma_{X_m} = \frac{\ln[1 + \rho_L(k, m)]}{\sqrt{\exp(\sigma_{X_k}^2) - 1}\sqrt{\exp(\sigma_{X_m}^2) - 1}} \quad (7)$$

The  $X_k(n)$  can be obtained from the white Gaussian random variables,  $W_k(n)$ , by using the following orthogonal transformation as

$$\begin{bmatrix} X_1(n) \\ X_2(n) \\ \dots \\ X_N(n) \end{bmatrix} = A \begin{bmatrix} W_1(n) \\ W_2(n) \\ \dots \\ W_N(n) \end{bmatrix} \quad (8)$$

where A is the transformation matrix which is obtained by decomposing the correlation matrix of  $X_k(n)$ .

The white Gaussian random variables can easily be generated by Box-Muller method<sup>(11)</sup>. Suzuki distributed random variable,  $A_k(n)$  is obtained by the PDF transformation of

$$A_k(n) = \sqrt{-2L_k(n) \ln(1 - U_{3k})} \quad (9)$$

where  $U_{3k}$  is an independent uniformly distributed random variable.

2. The Revised Algorithm for the Generation of Suzuki Fading Signal

It is necessary to modify the conventional procedure introduced in the previous section so that the lognormal fading component can have the spatial correlation between amplitudes in successive profiles. The lognormal fading components have the spatial correlation coefficient  $\rho_{Lk}(1)$  between the k-th paths in the adjacent profiles. At the same time, the lognormal fading components in a profile have the temporal correlation,  $\rho_L(k, m)$ , between path k and m. Fig. 4 shows the relationships between lognormal fading components.

The lognormal fading components between the k-th paths in adjacent profiles have the spatial correlation  $\rho_{Lk}(1)$  as

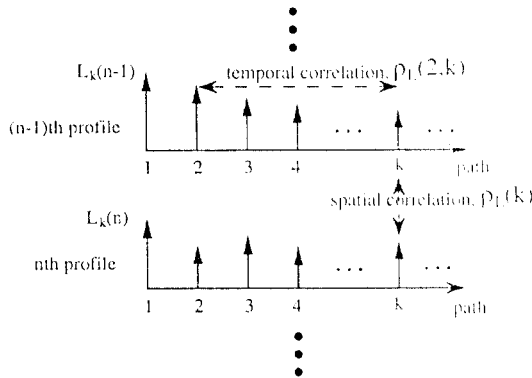


Fig. 4. Sequence of Profiles.

$$\rho_{L_k}(1) = E\{L_k(n)L_k(n-1)\}/\sigma_{L_k}^2$$

for  $k = 1, 2, \dots, N$  (10)

where  $\sigma_{L_k}^2$  is the variance of  $L_k(n)$  for all  $n$ . The correlated lognormally distributed random variables can be generated from the correlated Gaussian distributed random variables as the algorithm described in the previous section<sup>(6)</sup>. However, the spatially and temporally correlated  $L_k(n)$  can be generated from the spatially and temporally correlated  $X_k(n)$ . Hence,  $X_k(n)$  is required to have the spatial correlation  $\rho_{X_k}(1)$  as well as the temporal correlation  $\rho_X(k, m)$ . The relationship between  $\rho_{L_k}(k, m)$  and  $\rho_X(k, m)$  is given by the equation (7). Since  $\rho_{L_k}(1)$  represents the spatial correlation of  $L_k(n)$  between the  $k$ -th paths of the adjacent profiles, the corresponding  $\rho_{X_k}(1)$  represents the spatial correlation of the Gaussian random variable from which  $L_k(n)$  will be obtained. The relationship between  $\rho_{L_k}(1)$  and  $\rho_{X_k}(1)$  can be obtained by

$$\rho_{X_k}(1)\sigma_{X_k}^2 = \ln[1 + \rho_{L_k}(1)(\exp(\sigma_{X_k}^2) - 1)].$$
 (11)

The spatially and temporally correlated Gaussian random variable  $X_k(n)$  can be obtained from a Gaussian random variable of

which the mean is zero and the variance  $\sigma_{X_k}^2(1 - \rho_{X_k}^2(1))$  and temporal correlation  $\tilde{\rho}_X(k, m)$  with no spatial correlation by using a linear transformation

$$X_k(n) = \tilde{X}_k(n) + \rho_{X_k}(1)X_k(n-1).$$
 (12)

The temporally correlated  $\tilde{X}_k(n)$  can be obtained from the white Gaussian random variable  $W_k(n)$  as in the equation (8). The initial condition of equation (12) is given by

$$X_k(n) = \begin{cases} 0 & \text{for } n < 0 \\ X_k(0) & \text{for } n = 0 \end{cases}$$
 (13)

where  $X_k(0)$  is a Gaussian random variable of which the mean is zero and the variance  $\rho_{X_k}^2$  and the temporal correlation  $\rho_X(k, m)$ . The spatially, temporally correlated  $L_k(n)$  can be obtained by the equation (6) and the Suzuki fading signal is generated by the equation (9).

At this point, we should show the two things. The one is that  $X_k(n)$  has the spatial correlation  $\rho_{X_k}(1)$ . The PDF of  $\tilde{X}_k(n)$  is expressed as

$$p(\tilde{X}_k(n)) = \frac{1}{\sigma_{X_k}\sqrt{2\pi(1 - \rho_{X_k}^2(1))}} \exp\left[-\frac{\{\tilde{X}_k(n)\}^2}{2\sigma_{X_k}^2(1 - \rho_{X_k}^2(1))}\right].$$
 (14)

From the equation (12), it is possible to obtain the conditional PDF of the Gaussian random variable  $X_k(n)$  under the assumption that Gaussian random variable  $X_k(n-1)$  is constant. The joint PDF of  $X_k(n)$  and  $X_k(n-1)$  can be found from the conditional PDF of  $X_k(n)$  as

$$p(X_k(n), X_k(n-1)) = \frac{1}{\sigma_{X_k}\sqrt{2\pi(1 - \rho_{X_k}^2(1))}} \times \exp\left[-\frac{\{X_k^2(n) - 2\rho_{X_k}(1)X_k(n)X_k(n-1) + X_k^2(n-1)\}}{2\sigma_{X_k}^2(1 - \rho_{X_k}^2(1))}\right].$$
 (15)

Thus, it is apparent that  $X_k(n)$  has the spatial correlation  $\rho_{X_k}(1)$  between adjacent

profiles from the equation (15). The spatial correlation between the n-th profile and the (n-1)-th profile can be written as

$$\rho_{X_k}(1) = \rho_{X_k}^l(1). \tag{16}$$

The other is that  $X_k(n)$  has the temporal correlation as

$$E\{X_k(n)X_m(n)\} = \rho_X(k, m)\sigma_{X_k}\sigma_{X_m}. \tag{17}$$

Suppose the temporal correlation of  $\tilde{X}_k(n)$  is

$$\rho_{\tilde{X}_k}(k, m) = \rho_{X_k}(k, m) \frac{1 - \rho_{X_k}(1)\rho_{X_m}(1)}{\sqrt{1 - \rho_{X_k}^2(1)}\sqrt{1 - \rho_{X_m}^2(1)}}. \tag{18}$$

First, we calculate

$$\begin{aligned} E\{X_k(n)X_m(n)\} &= E\{\tilde{X}_k(n) + \rho_{X_k}(1)X_k(n-1) \\ &\quad (\tilde{X}_m(n) + \rho_{X_m}(1)X_m(n-1))\} \\ &= E\{\tilde{X}_k(n)\tilde{X}_m(n)\} + \rho_{X_k}(1)\rho_{X_m}(1) \\ &\quad E\{X_k(n-1)X_m(n-1)\} \\ &\quad + \rho_{X_k}(1)E\{X_k(n-1)\tilde{X}_m(n)\} \\ &\quad + \rho_{X_m}(1)E\{X_m(n-1)\tilde{X}_k(n)\}. \end{aligned} \tag{19}$$

$\tilde{X}_k(n)$  and  $\tilde{X}_m(n)$  are independent of profile index n and the initial value  $X_k(0)$  is generated to be independent of  $\tilde{X}_m(n)$  for any path k, m. Therefore, the expectation of  $X_m(n-1)\tilde{X}_k(n)$  and that of  $X_k(n-1)\tilde{X}_m(n)$  are all zero, which are appeared in the third and the fourth term in the equation (19). The equation (19) becomes,

$$\begin{aligned} E\{\tilde{X}_k(n)\tilde{X}_m(n)\} + \rho_{X_k}(1)\rho_{X_m}(1)E\{X_k(n-1) \\ X_m(n-1)\} &= \rho_{\tilde{X}_k}(k, m)\sqrt{1 - \rho_{X_k}^2(n, k)} \\ &\quad \sigma_{X_k}\sqrt{1 - \rho_{X_m}^2(n, m)}\sigma_{X_m} + \rho_{X_k}(1)\rho_{X_m}(1) \\ &\quad E\{X_k(n-1)X_m(n-1)\} \end{aligned} \tag{20}$$

Using equation (18), the equation (20) becomes equation (17). Thus, with the equation (18),  $X_k(n)$  has the temporal correlation of the equation (17).

The  $\rho_X(k, m)$  is determined by the equation (7) and the equation (18) with the given  $\rho_L(k, m)$  and  $\rho_{X_k}(1)$  is determined by the equation (11), the spatially, temporally completed  $X_k(n)$  can be generated by the derived method.

### 3. The Extended Algorithm for the Generation of Suzuki Fading Signal when the Diversity Receiver is used

Most base stations use a diversity receiver to cope with the faded signal<sup>(6)</sup>. Mobile stations also adopts the diversity receiver in most cases. Thus diversity receiver can be regarded as a part of mobile communications channel. In the section III.2, we have derived the algorithm that generates the spatially, temporally correlated lognormal fading component. However, the Rayleigh fading component is generated by using the same method of the reference [5] for the channel where a single antenna is used. In this section, we derive the method that generates the Rayleigh fading components at each diversity antenna have the correlation corresponding to the antenna spacing.

We assume that lognormal fading components are almost completely correlated such that

$$L_k = L_{k1} \approx L_{k2}$$

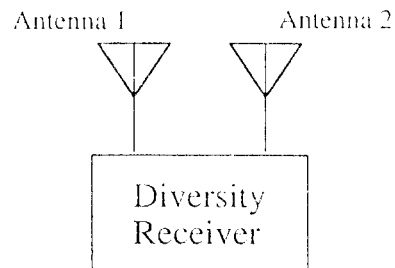


Fig. 5. 2-branch Diversity Receiver.



where  $L_{k1}$  is the lognormal fading component of antenna 1 and  $L_{k2}$  is that of antenna 2 and Rayleigh fading components at each diversity antenna have correlation coefficient,  $\rho_{Rk}(d)$  which is dependent on the antenna spacing  $d$ . The performance enhancement is the highest when two branches of diversity receiver are used. Using more branches brings smaller enhancement so in a practical situation only two branches are usually used<sup>(12)</sup>. In this section two branches are used. The correlation coefficients of Rayleigh fading component at the base station are measured at versatile situation. Table 3 gives the example values at the correlation coefficient of Rayleigh fading components when the diversity antenna are separated horizontally and vertically<sup>(9)</sup>.

Table 3. Measured Correlation Coefficient of Rayleigh Fading Component at Base Station.

SPACING		VERTICAL	HORIZONTAL
ANTENNA	3.4λ	0.714	0.712
SEPARATION	6.6λ	0.947	0.57
DISTANCE	10.0λ	0.722	0.432

We need two Rayleigh random variables for each diversity antenna which have correlation coefficient  $\rho_{Rk}(d)$ . If we denote Rayleigh fading component at the antenna 1 as  $R_{k1}$  and at the antenna 2 as  $R_{k2}$ , the correlation coefficient of these variables can be expressed as

$$\rho_{Rk}(d) = \frac{E[R_{k1}R_{k2}] - E[R_{k1}]E[R_{k2}]}{\sqrt{E[R_{k1}^2] - E^2[R_{k1}]}\sqrt{E[R_{k2}^2] - E^2[R_{k2}]}} \quad (2)$$

Rayleigh fading components can be obtained from the envelope of complex Gaussian random variables. Let the complex Gaussian random variable be  $(X_{k1}, Y_{k1})$  and  $(X_{k2}, Y_{k2})$ . The correlations of  $(X_{k1}, Y_{k1})$  and  $(X_{k2}, Y_{k2})$  are assumed as follows:

$$\begin{aligned} E[X_{k1}^2] &= E[Y_{k1}^2] = \sigma_{Xk1}^2, \quad E[X_{k2}^2] = E[Y_{k2}^2] = \sigma_{Xk2}^2 \\ E[X_{k1}X_{k2}] &= E[X_{k2}X_{k1}] = E[Y_{k1}Y_{k2}] \\ &= E[Y_{k2}Y_{k1}] = \sigma_{Xk1}\sigma_{Xk2}\rho_{Xk}(d) \quad (22) \\ E[X_{k1}Y_{k1}] &= E[Y_{k1}X_{k1}] = E[X_{k2}Y_{k2}] = E[Y_{k2}X_{k2}] = 0 \\ E[X_{k1}Y_{k2}] &= E[Y_{k2}X_{k1}] = E[X_{k2}Y_{k1}] = E[Y_{k1}X_{k2}] = 0. \end{aligned}$$

The relation between  $\rho_{Rk}(d)$  and the correlation coefficient of two sets of Gaussian random variables,  $(X_{k1}, Y_{k1})$  and  $(X_{k2}, Y_{k2})$ , is given by<sup>(12)</sup>

$$\rho_{Rk}(d) = \frac{\pi}{4(4-\pi)} \rho_{Xk}^2(d). \quad (23)$$

From the equation (22), we can write the fourth order Gaussian PDF of  $(X_{k1}, Y_{k1})$  and  $(X_{k2}, Y_{k2})$  as

$$\begin{aligned} p(X_{k1}, Y_{k1}, X_{k2}, Y_{k2}) &= \frac{1}{4\pi^2 \sigma_{Xk1}^2 \sigma_{Xk2}^2 (1 - \rho_{Xk}^2(d))} \\ &\exp\left[ -\frac{1}{2(1 - \rho_{Xk}^2(d))} \times \left\{ (X_{k1}/\sigma_{Xk1})^2 - 2(\rho_{Xk}(d) / \sigma_{Xk1}\sigma_{Xk2}) X_{k1}X_{k2} + (X_{k2}/\sigma_{Xk2})^2 \right. \right. \\ &\quad \left. \left. + (Y_{k1}/\sigma_{Xk1})^2 - 2(\rho_{Xk}(d) / \sigma_{Xk1}\sigma_{Xk2}) Y_{k1}Y_{k2} + (Y_{k2}/\sigma_{Xk2})^2 \right\} \right]. \quad (24) \end{aligned}$$

This fourth order Gaussian density can be transformed to  $p(R_{k1}, R_{k2}, \phi_{k1}, \phi_{k2})$  such that

$$\begin{aligned} R_{k1} &= \sqrt{X_{k1}^2 + Y_{k1}^2}, \quad \phi_{k1} = \arctan(Y_{k1}/X_{k1}) \\ R_{k2} &= \sqrt{X_{k2}^2 + Y_{k2}^2}, \quad \phi_{k2} = \arctan(Y_{k2}/X_{k2}). \quad (25) \end{aligned}$$

So the transformed PDF is

$$\begin{aligned} p(R_{k1}, R_{k2}, \phi_{k1}, \phi_{k2}) &= |J_1| p(X_{k1}, Y_{k1}, X_{k2}, Y_{k2}) \\ &= \frac{R_{k1}R_{k2}}{4\pi^2 \sigma_{Xk1}^2 \sigma_{Xk2}^2 (1 - \rho_{Xk}^2(d))} \exp\left[ \frac{-1}{2(1 - \rho_{Xk}^2(d))} \right. \\ &\quad \left. \times \{ R_{k1}^2 / \sigma_{Xk1}^2 + R_{k2}^2 / \sigma_{Xk2}^2 - 2(\rho_{Xk}(d) / \sigma_{Xk1}\sigma_{Xk2}) \right. \\ &\quad \left. R_{k1}R_{k2} \cos(\phi_{k2} - \phi_{k1}) \right] \quad (26) \end{aligned}$$

where  $J_1$  is the jacobian of the transformation (25). The joint PDF of Rayleigh random variables is obtained by integrating the equation (26) with respect to  $\phi_{k1}$  and  $\phi_{k2}$ <sup>(12)</sup> as

$$\begin{aligned} p(R_{k1}, R_{k2}) &= \int_0^{2\pi} \int_0^{2\pi} p(R_{k1}, R_{k2}, \phi_{k1}, \phi_{k2}) d\phi_{k1} d\phi_{k2} \\ &= \frac{R_{k1}R_{k2}}{\sigma_{X1}^2\sigma_{X2}^2(1-\rho_{Xk}^2(d))} \times \exp\left[ \right. \\ &\quad \left. -\frac{R_{k1}^2/\sigma_{X1}^2 + R_{k2}^2/\sigma_{X2}^2}{2\sigma_{X1}^2\sigma_{X2}^2(1-\rho_{Xk}^2(d))} \right] I_0\left[ \frac{R_{k1}R_{k2}\rho_{Xk}(d)}{\sigma_{X1}\sigma_{X2}(1-\rho_{Xk}^2(d))} \right]. \end{aligned} \quad (27)$$

The relation between  $\rho_{Rk}(d)$  and  $\rho_{Xk}(d)$  can be found by using the mean and variance of Rayleigh random variables and expectation of  $R_{k1}R_{k2}^{(12)}$  as

$$\rho_{Rk}(d) = \frac{E[R_{k1}R_{k2}] - E[R_{k1}]E[R_{k2}]}{\sqrt{E[R_{k1}^2] - E[R_{k1}]^2} \sqrt{E[R_{k2}^2] - E[R_{k2}]^2}} \quad (28)$$

and it becomes the equation (23).

Since we know the relation of  $\rho_{Xk}(d)$  and  $\rho_{Rk}(d)$  as the equation (23), the two correlated Rayleigh random variables with any correla-

tion coefficient can be obtained from four correlated Gaussian random variables. The four correlated Gaussian random variables can be generated by transforming the independent Gaussian random variables ( $W_{k1}, Z_{k1}$ ) and ( $W_{k2}, Z_{k2}$ ) using

$$\begin{aligned} \begin{pmatrix} X_{k1} \\ X_{k2} \end{pmatrix} &= \begin{pmatrix} \sigma_{Xk}\sqrt{(1+\rho_{Xk}(k,d))/\sqrt{2}} \\ \sigma_{Xk}\sqrt{(1+\rho_{Xk}(k,d))/\sqrt{2}} \\ -\sigma_{Xk}\sqrt{(1-\rho_{Xk}(k,d))/\sqrt{2}} \\ \sigma_{Xk}\sqrt{(1-\rho_{Xk}(k,d))/\sqrt{2}} \end{pmatrix} \begin{pmatrix} W_{k1} \\ W_{k2} \end{pmatrix} \\ \begin{pmatrix} Y_{k1} \\ Y_{k2} \end{pmatrix} &= \begin{pmatrix} \sigma_{Xk}\sqrt{(1+\rho_{Xk}(k,d))/\sqrt{2}} \\ \sigma_{Xk}\sqrt{(1+\rho_{Xk}(k,d))/\sqrt{2}} \\ -\sigma_{Xk}\sqrt{(1-\rho_{Xk}(k,d))/\sqrt{2}} \\ \sigma_{Xk}\sqrt{(1-\rho_{Xk}(k,d))/\sqrt{2}} \end{pmatrix} \begin{pmatrix} Z_{k1} \\ Z_{k2} \end{pmatrix}. \end{aligned} \quad (29)$$

From the PDF of ( $X_{k1}, Y_{k1}$ ), ( $X_{k2}, Y_{k2}$ ), the PDF of the independent Gaussian random

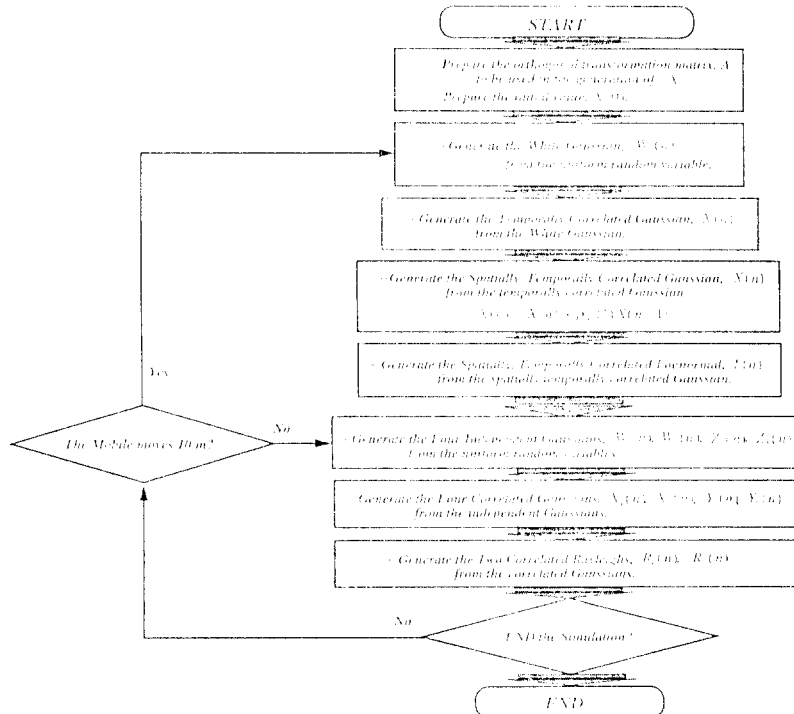


Fig. 6. Flow Chart of the Expanded Algorithm.

variables  $(W_{k1}, Z_{k1}), (W_{k2}, Z_{k2})$  can be obtained as

$$p(W_{k1}, Z_{k1}, W_{k2}, Z_{k2}) = p(X_{k1}, Y_{k1}, X_{k2}, Y_{k2}) | J_2 |$$

$$= \frac{1}{4\pi^2} \exp\left[ -\frac{1}{2} (W_{k1}^2 + W_{k2}^2 + Z_{k1}^2 + Z_{k2}^2) \right] \quad (30)$$

where  $J_2$  is the jacobian of transformation (29).

The independent Gaussian random variables can easily be generated from the uniform random variables  $U_{k4}, U_{k5}, U_{k6}, U_{k7}$  <sup>(11)</sup> as

$$W_{k1} = \sqrt{-2 \ln U_{k4}} \cos(2\pi U_{k5})$$

$$W_{k2} = \sqrt{-2 \ln U_{k4}} \sin(2\pi U_{k5})$$

$$Z_{k1} = \sqrt{-2 \ln U_{k6}} \cos(2\pi U_{k7}) \quad (31)$$

$$Z_{k2} = \sqrt{-2 \ln U_{k6}} \sin(2\pi U_{k7}).$$

Consequently, using the equations (25), (29) and (31), we can get the correlated Rayleigh random variables from the independent uniform random variables. Thus if the generated lognormal fading component in the section III.2 is used as an average power, the  $R_{k1}$  and  $R_{k2}$  become Suzuki distributed random variables. The generated Suzuki fading signal is composed of Rayleigh fading component which have the spatial correlation depending on the diversity antenna spacing and the lognormal fading components which have the spatial correlation and the temporal correlation corresponding to the channel characteristics. Fig. 6 is the flow chart of the algorithm which is derived in the sections III.2 and III.3.

#### IV. Numerical Results and Discussion

The channel parameters and the temporal correlation values used in the simulation are given in Table 1 and Table 2 respectively. It has been assumed that carrier frequency is 900MHz and the lognormal fading component

is refreshed whenever a mobile moves a distance of 10m. The spatial correlation coefficient of 0.89 is used for all paths in the simulation and the value represent the correlation when a mobile receiver moves a distance of 10m. The value is roughly calculated from the measured data <sup>(4)</sup>.

Fig. 7 shows the cumulative distribution function (CDF) of the Suzuki fading strength generated with the proposed algorithm and that of the theoretical values for paths 1, 2, 3 and 7. The generated fading path strengths almost agree with the theoretical values. The theoretical values of CDF for path k is obtained by <sup>(12)</sup>

$$CDF(A_k) = \int_0^{\infty} (1 - \exp(-\frac{A_k^2}{2L_k})) \frac{10 \log_{10} e}{\sqrt{2\pi} \sigma_{L_k} L_k}$$

$$\times \exp\left[ -\frac{\{10 \log_{10}(L_k/\lambda_k)\}^2}{2\sigma_{L_k}^2} \right] dL_k. \quad (32)$$

Fig. 8. compares the simulated values of the spatial correlation coefficient of lognormal fading component to empirical values. And Fig. 9. shows the temporal correlation coefficient with the corresponding empirical values. The simulated correlation coefficient is obtained by using <sup>(13)</sup>

$$\rho_X(k, m) = \frac{\sum_{n=1}^M (X_k(n) - \bar{X}_k)(X_m(n) - \bar{X}_m)}{\sqrt{\sum_{n=1}^M (X_k(n) - \bar{X}_k)^2 \sum_{n=1}^M (X_m(n) - \bar{X}_m)^2}} \quad (33)$$

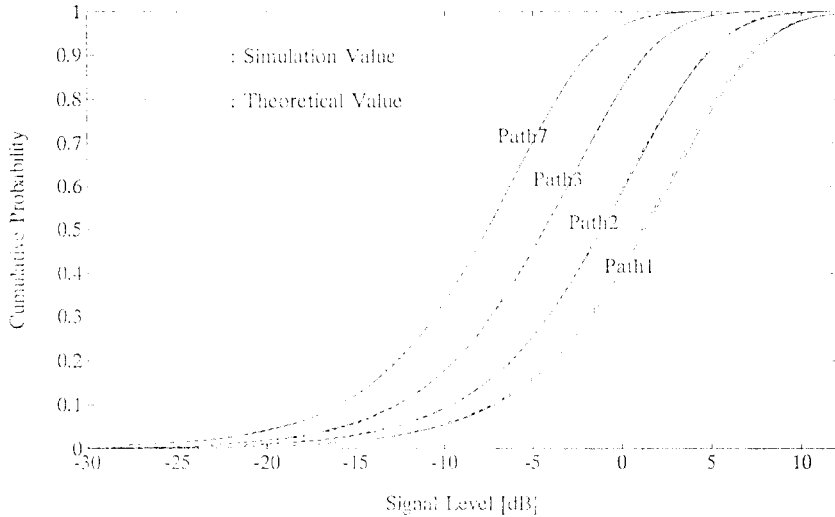
The correlation coefficients almost agree with the empirical values except some error appearing in the temporal correlation. In the equation (18) the third and the fourth term are assumed to be zero. These terms can be expressed as

$$\rho_{Xk}(1) E\{X_k(n-1) \tilde{X}_m(n)\}$$

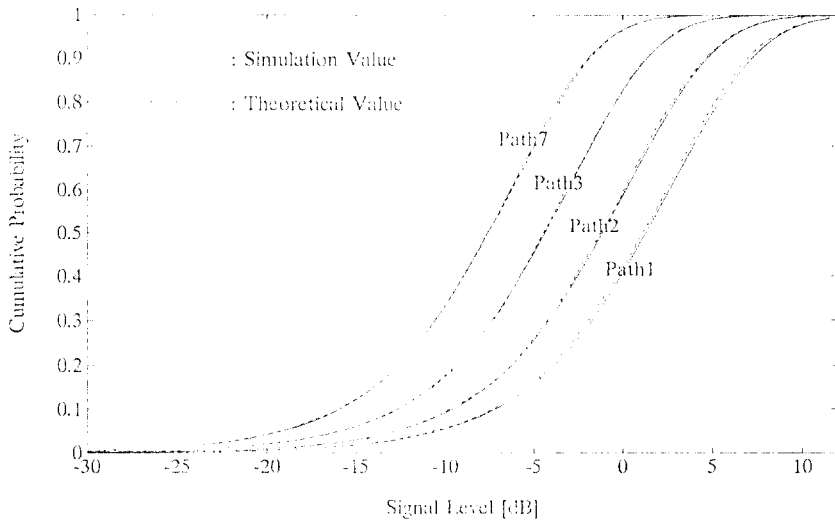
$$= \rho_{Xk}(1) E\{ \tilde{X}_k(n-1) + \rho_{Xk}(1) X_k(n-2) \} \tilde{X}_m(n)$$

$$\begin{aligned}
 &= \rho_{\tilde{X}_k}(1) E\{\tilde{X}_k^*(n-1)\tilde{X}_k^*(n)\} + \rho_{\tilde{X}_m}^2(1) E\{X_k(n-2) \\
 &\quad \tilde{X}_m^*(n)\} \\
 &= \dots \\
 &= \sum_{i=1}^n \rho_{\tilde{X}_i}^2(1) E\{\tilde{X}_i^*(n-i)\tilde{X}_i^*(n)\}.
 \end{aligned}
 \tag{34}$$

The third and fourth term of the equation (18) are expressed as the summation of  $E\{\tilde{X}_k(n)\tilde{X}_m(n-i)\}$ . The accumulation of these values is unavoidable and it causes the temporal correlation values to have the small



(a) Suzuki Distribution for Diversity Antenna 1



(b) Suzuki Distribution for Diversity Antenna 2

Fig. 7. Cumulative Distribution Function of Suzuki Fading Signals, number of sample = 5000,  $\lambda_1 = 1.000$ ,  $\sigma_1 = 2.0277$ ,  $\lambda_2 = 0.5708$ ,  $\sigma_2 = 1.9253$ ,  $\lambda_3 = 0.2698$ ,  $\sigma_3 = 1.6982$ ,  $\lambda_7 = 0.1281$ ,  $\sigma_7 = 1.5560$ .

deviation.

The correlation coefficient of Rayleigh fading component is plotted in Fig. 10. The simulation values deviate from the theoretical values when the correlation coefficient value

is large. When the equation (23) is evaluated<sup>(12)</sup>, the expectation of  $R_{k1}R_{k2}$  is approximated by a series expansion and the high order terms of the series are neglected. This causes the deviation of correlation coefficients.

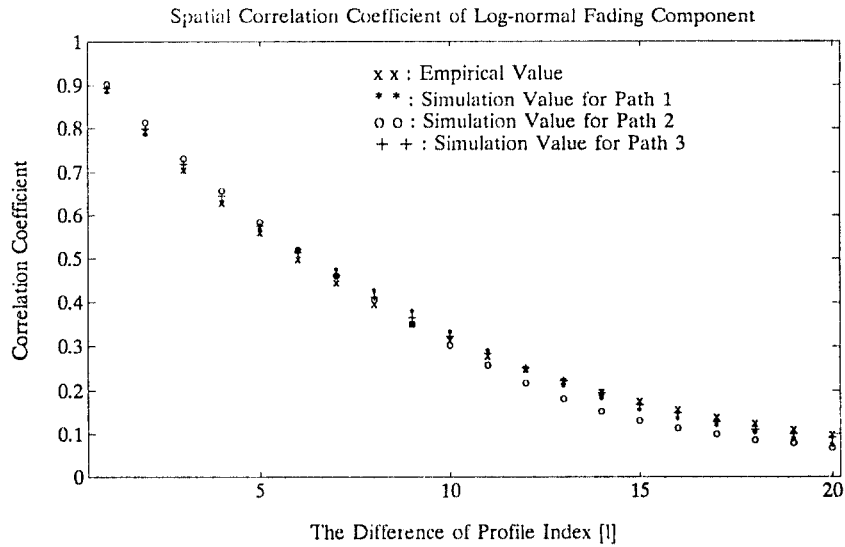


Fig. 8. Spatial Correlation Coefficient of Lognormal Fading Component, number of sample = 5000.

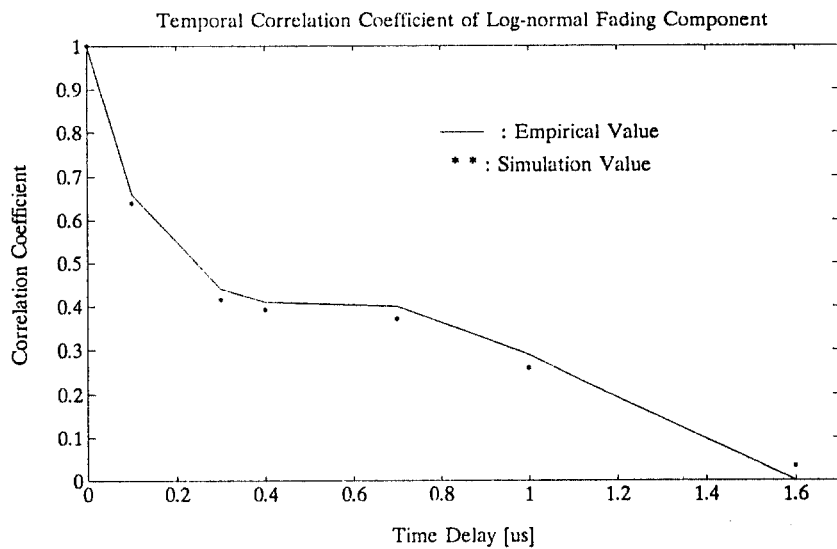


Fig. 9. Temporal Correlation Coefficient of Lognormal Fading Component, number of sample = 5000.

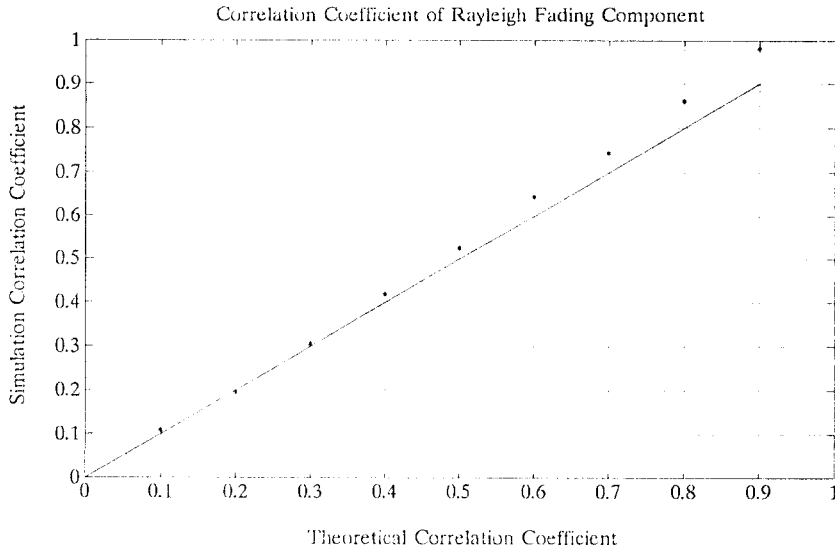


Fig. 10. Correlation Coefficient of Rayleigh Fading Component.

$$\begin{aligned}
 E\{R_{k1}R_{k2}\} &= \frac{\pi}{2} \sigma_{XR1}\sigma_{XR2} [1 + (\frac{1}{2})^2 \rho_X^2(k, d) \\
 &+ (\frac{1}{2})^6 \rho_X^4(k, d) + \dots] \\
 &\approx \frac{\pi}{2} \sigma_{XR1}\sigma_{XR2} [1 + (\frac{1}{2})^2 \rho_X^2(k, d)]
 \end{aligned}
 \tag{35}$$

The proposed algorithm can generate the Suzuki fading signal and it can control the spatial correlation of the lognormal fading component between amplitudes in the adjacent profiles and the temporal correlation between paths in a profile. The algorithm can also be applicable when a diversity receiver is used.

### V. CONCLUSION

We have proposed the improved mobile channel simulation algorithm which generates the Suzuki fading signals. The spatial correlation of lognormal fading component in addition to the temporal correlation is taken into account. The temporal correlation of lognor-

mal fading component is considered for all paths within the range of 1  $\mu$ s. in contrast with the conventional algorithm<sup>(3)</sup> which considers consecutive paths only. It has been shown that the algorithm can be extended for the simulation of the multipath fading channel where a diversity receiver is used. With the proposed algorithm, the correlations of Suzuki fading signal can easily be controllable. Therefore, more realistic multipath fading channel simulation is possible.

The wide-band mobile communication systems are required in many applications such as cordless telephone, personal communication networks, mobile-satellite communications and etc. The proposed algorithm can be used not only in the estimation of existing system performance, but also in the design of urban communication systems.

REFERENCE

1. G. L. Turin, F. D. Clapp, T. L. Johnston, S. B. Fine and D. Lavry, "A statistical model of urban multipath propagation," IEEE Trans. Veh. Technol., vol. 21, pp.1-9, Feb. 1972.
2. H. Suzuki, "A statistical model for urban radio propagation," IEEE Trans. Commun., vol. 25, pp.673-680, July 1977.
3. H. Hashemi, "Simulation of the urban radio propagation channel," IEEE Trans. Veh. Technol., vol. 28, pp.213-225, Aug. 1979.
4. A. M. D. Turkmani, D. A. Demery and J. D. Parsons, "Measurement and modeling of wide-band mobile radio channels at 900 MHz," IEE Proc. I, vol. 138, pp.447-457, Oct. 1991.
5. T. J. Park, Y. S. Park, H. M. Kim, "Wide-band Cannel Simulation Algorithm for the Suzuki Fading Channel" The Journal of the Korean Institute of Communication Sciences, Vol. 19, No. 8, pp.1493-1502, Aug. 1994
6. N. J. Boucher, The Cellular Radio Handbook, Mendocino, Quantum Publishing, 1990.
7. W. C. Y. Lee, "Effects on correlation between two mobile radio base station antennas," IEEE Trans. Commun., vol. 21, pp.1214-1224, Nov. 1973.
8. F. Adachi, M. T. Feeney, A. G. Williamson and J. D. Parsons, "Crosscorrelation between the envelopes of 900MHz signals received at a mobile radio base station site," IEE Proc. F, vol. 133, pp.506-512, Oct. 1986.
9. S. B. Rhee, G. I. Zysman, "Results of suburban base station spatial diversity measurement in the UHF band," IEEE Trans. Commun., Vol. 22, pp.1630-1636, Oct. 1974.
10. J. D. Parsons, The Mobile Radio Propagation Channel, New York, Wiley, 1992.
11. A. Papoulis, Probability, Random Variables, And Stochastic Processes, New York, McGraw-Hill, 1991.
12. Michel Daoud Yacoub, Foundations of Mobile Radio Engineering, Boca Raton, CRC Press, 1993.
13. J. W. Daniel, Applied Linear Algebra, New Jersey, Prentice-Hall, 1988.



張眞元(Jin Weon Chang) 정회원

1971년 1월 9일생

1993년 2월 : 한국과학기술원 전기 및 전자공학과 학사

1995년 2월 : 한국과학기술원 전기 및 전자공학과 석사

1995년 2월~현재 : 한국과학기술원 전기 및 전자공학과 박사 과정

※주관심 분야 : 이동통신, CDMA 시스템, Wireless Network.



朴洋守(Yang Soo Park) 정회원

1965년 10월 22일생

1988년 2월 : 한국항공대학교 항공전자공학과(공학사)

1990년 2월 : 한국과학기술원 전기 및 전자공학과(공학석사)

1990년 3월~1992년 8월 : 한국통신 서울전차교환운용연구단 전임연구원

1992년 9월~현재 : 한국과학기술원 전기 및 전자공학과 박사 과정

※주관심 분야 : 디지털신호처리, 최적신호처리, 이동통신시스템

## 河 求 睿(Ku Yong Ha)

정회원

1987년 2월 : 부산대학교 전자공학과(학사)  
 1989년 2월 : 한국과학기술원 전기 및 전자공학과(석사)  
 1992년 3월~현재 : 한국과학기술원 전기 및 전자공학과 박사  
 과정



## 金 炯 明(Hyung Myung Kim) 정회원

1952년 10월 24일생  
 1982년 2월 : 서울대학교 공학사  
 1982년 4월 : 미국 Pittsburgh 대  
 학 전기공학사 석사  
 1985년 12월 : 미국 Pittsburgh 대  
 학 전기공학과 공학박  
 사  
 1986년 4월~1992년 8월 : 한국과학기술원 전기 및 전자공학  
 과 조교수  
 1992년 9월~현재 : 한국과학기술원 전기 및 전자공학과 부교수  
 ※주관심 분야 : 디지털 신호와 영상처리, 다차원시스템 이론,  
 비디오신호 전송통신 이론, 이동 통신 기술  
 분야